Analytic Modeling of Monolithic Inductors on Semiconductor Substrates

Seung-Jin Yoo, Rob Friar, and Dean P. Neikirk
Microelectronics Research Center and EERL
Dept. of Electrical and Computer Engineering,
Mail Code R9900, The University of Texas at Austin, Austin, TX 78712;
phone: (512) 471-8104, FAX (512) 471-8575;
e-mail: yoosj@happy.cc.utexas.edu

Abstract: For inductors on silicon substrates a simple, predictive model is presented that explicitly accounts for substrate resistivity. Model and experimental results are in excellent agreement over a wide range of geometries, semiconductor resistivities, and frequency.

Introduction: There have been many equivalent circuit models proposed to describe the behavior of planar spiral inductors on silicon substrates (for example, [1]). The generic topology of these circuits are all very similar (Fig. 1), but in almost all cases the models are used to fit experimentally measured data (e.g., [2-5]), and hence are of limited use for design purposes. Most predictive models are essentially the same as those used by Dill, Gleason, and Greenhouse [6-8]; all such methods are ultimately based on the calculation of "partial inductances," most commonly attributed to Rosa and Grover [9-13]. A particular problem in modeling inductors on silicon with these techniques is the difficulty they have in dealing with frequency and resistivity dependent current distribution in the relatively thick silicon substrate itself. Of the components illustrated in Fig. 1, the substrate resistivity can affect the values assigned to L_{series}, R_{series}, C_{semi}, and G_{semi}.

For MIS inductors (i.e., inductors fabricated on an insulator-coated semiconductor substrate) a new, simple, predictive model is presented here that quantitatively accounts for the effect of substrate resistivity, which is critical in the accurate prediction of inductor characteristics. Given the geometry, substrate resistivity, and dielectric constants used in the structure, our model predicts the frequency dependent resistance, inductance, and capacitance of a planar inductor using closed-form formulas. No curve fitting is used in our new model. Hence, this model can be used efficiently for the design and analysis of planar thin film inductors on semiconductor substrates. Model results and experimental measurements are in excellent agreement for a wide range of test geometries, semiconductor substrate resistivities, and frequency.

Model: An inductor fabricated on an oxide-on-silicon substrate can be modeled as a collection of short microstrip transmission line sections that are affected by both the substrate and the global geometry of the entire inductor. For the microstrip-like behavior, our group has already developed an excellent model that accurately and efficiently predicts the impact of substrate resistivity and frequency on the series impedance of the microstrip [14]. However, when applying this model to planar inductors, an additional frequency independent mutual inductance from the geometry of the coils must be included. The model assumes a rectangular or square shaped inductor. The mutual inductance can be calculated between parallel conducting metal segments by using Greenhouse methods [8]. The self-reactance (both the inductive and capacitive components) is approximated using our quasi-static model of microstrip lines on a semiconducting substrate [14].

Model verification: In order to verify the accuracy of our inductor model we have fabricated several "primitive" test geometries; these geometries represent extremes of line-to-line and line-to-substrate coupling to help determine the robustness of our approach. Here we show a comparison between measured and modeled results for three different one turn spiral inductors, on both "low" (3.8Ω-cm) and "high" (20Ω-cm; higher values become even easier to model) resistivity silicon substrates (500μm thick) covered with 0.45μm of thermal oxide. For all three geometries the overall length (4750μm), linewidth (50μm), and metal thickness (0.9μm) are the same; hence, the DC resistance of all the coils is the same.

The first primitive geometry studied is a simple square; in this structure the mutual inductances will be fairly small, and the MIS microstrip behavior of the lines would be expected to dominate. The second geometry is a long rectangle with moderately spaced lines; this case should have moderately sized mutuals with large MIS effects. The third geometry is a pair of closely spaced lines; in this case the impact of mutual inductance should be large, but MIS effects are still critical in determining the high frequency behavior of the loop.

0-7803-4965-2/98/$10.00©1998 IEEE

As shown below, our predictive model is in good agreement with measurement for both the real and imaginary parts of the loop impedance over a wide frequency range, including frequencies approaching and exceeding the self-resonance frequency. Note that our model and measurements indicate the critical role of substrate resistivity in determining the high frequency behavior near self-resonance. To capture such effects using models based on parameter extraction from measured data, the fabrication of many test structures on many different resistivity substrates would be required. For design purposes, this emphasizes the utility of inductor models, such as the one presented here, that quantitatively incorporate substrate resistivity.

[1] C. P. Yue, C. R. Ryu, J. Lau, T. Lee, and S. Wong, "A Physical Model for Planar Spiral Inductors on Silicon," IEEE International Electron Devices Meeting, , 1996, pp. 155-158.
[2] Y. C. Shih, C. K. Pao, and T. Itoh, "A broadband parameter extraction technique for the equivalent circuit of planar inductors," IEEE MTT-S International Microwave Symposium, Vol. 3, , 1992, pp. 1345-1348.
[3] J. Zhao, R. Frye, W. Dai, and K. Tai, "S Parameter-Based Experimental Modeling of High Q MCM Inductor with Exponential Gradient Learning Algorithm," *IEEE Transactions on Components, Packaging, and Manufacturing Technology - Part B: Advanced Packaging*, vol. 20, pp. 202-210, 1997.
[4] S. F. Mahmoud and E. Beyne, "Inductance and Quality-Factor Evaluation of Planar Lumped Inductors in a Multilayer Configuration," *IEEE Transactions on Microwave Theory and Techniques*, vol. 45, pp. 918-923, 1997.
[5] R. A. Johnson, C. E. Chang, P. M. Asbeck, M. E. Wood, G. A. Garcia, and I. Lagnado, "Comparison of Microwave Inductors Fabricated on Silicon-on-Sapphire and Bulk Silicon," *IEEE Microwave and Guided Wave Letters*, vol. 6, pp. 323-325, 1996.
[6] H. G. Dill, "Designing Inductors for Thin-film Applications," in *Electronic Design*, 1964, pp. 52.
[7] F. R. Gleason, "Thin Film Microelectronic Inductors," National Electronics Conference, Chicago, 1964, pp. 197.
[8] H. M. Greenhouse, "Design of Planar Rectangular Microelectronic Inductors," *IEEE Transactions on Parts, Hybrids, and Packaging*, vol. Vol. PHP-10, 1974.
[9] E. B. Rosa, "Calculation of the Self-Inductance of single-Layer Coils," *Bulletin of the National Bureau of Standards*, vol. 2, pp. 161-187, 1906.
[10] E. B. Rosa, "On the Geometrical Mean Distance of Rectangular Areas and the Calculation of Self-Inductance," *Bulletin of the National Bureau of Standards*, vol. 3, pp. 1-41, 1907.
[11] E. B. Rosa, "The self and mutual inductances of linear conductors," *Bulletin of the National Bureau of Standards*, vol. 4, pp. 301-344, 1908.
[12] F. W. Grover, "The Calculation of the Inductance of Single-Layer Coils and Spirals Wound with Wire of Large Cross Section," *Proceedings of the Institute of Radio Engineers*, vol. 17, pp. 2053-2063, 1929.
[13] F. Grover, *Inductance Calculations, Working Formulas and Tables*. New York: Dover, 1962.
[14] E. Tuncer and D. P. Neikirk, "Highly Accurate Quasi-Static Modeling of Microstrip Lines Over Lossy Substrates," *IEEE Microwave and Guided Wave Letters*, vol. 2, pp. 409-411, 1992.

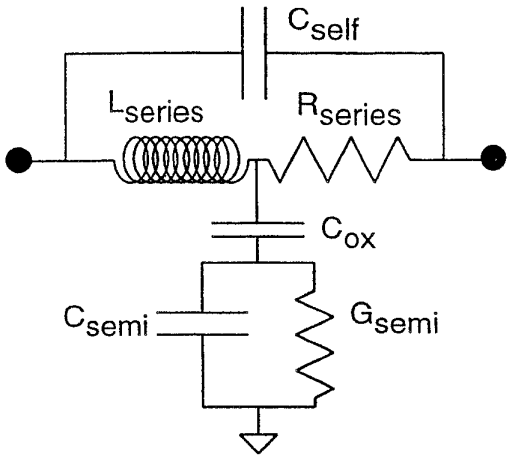

Figure 1: General circuit topology commonly used to model planar inductors on a semiconducting substrate.

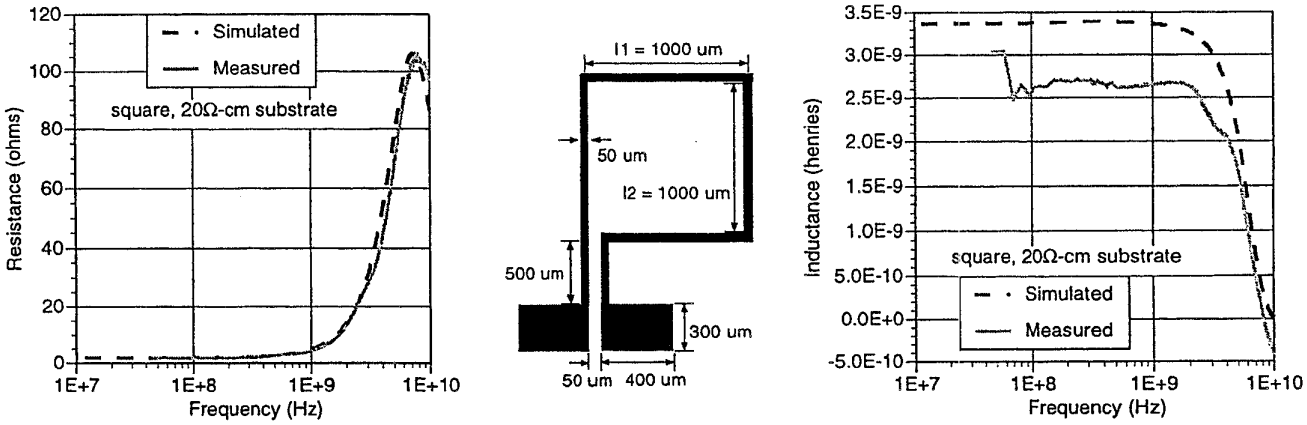

Figure 2: Microwave data (extracted from measured S-parameters) compared to new model for square test structure on a high resistivity (20Ω-cm) substrate.

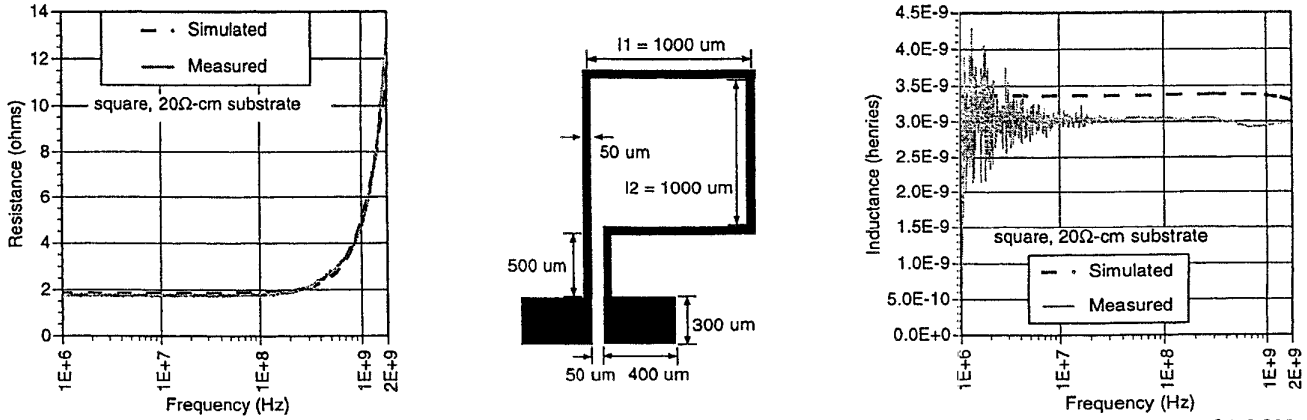

Figure 3: Comparison of simulated and data measured using vector impedance analyzer with maximum frequency of 1.8GHz, for square test structure on a high resistivity (20Ω-cm) substrate.

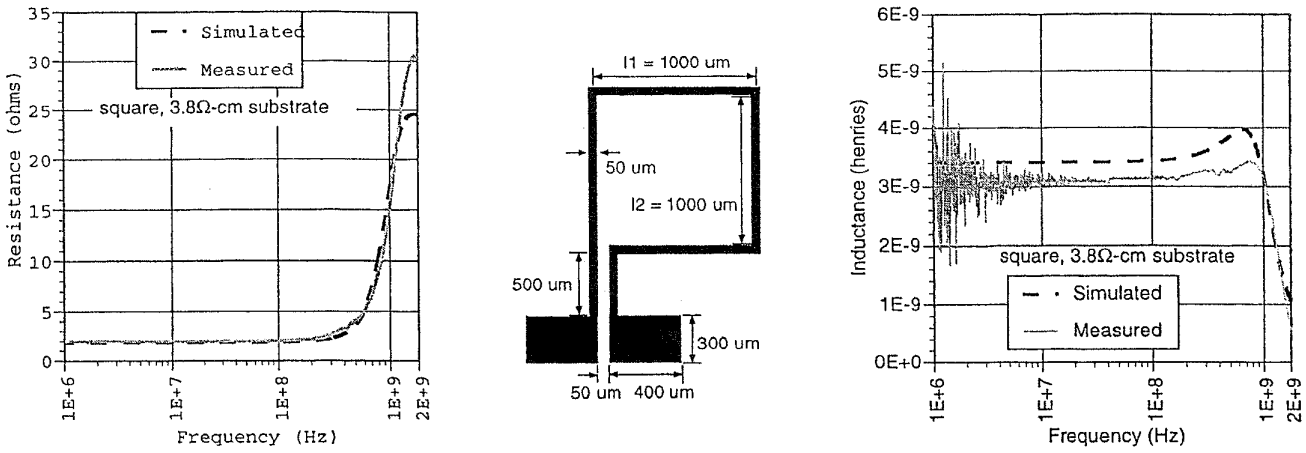

Figure 4: Comparison between simulation and measurement for square test structure on low resistivity (3.8Ω-cm) substrate.

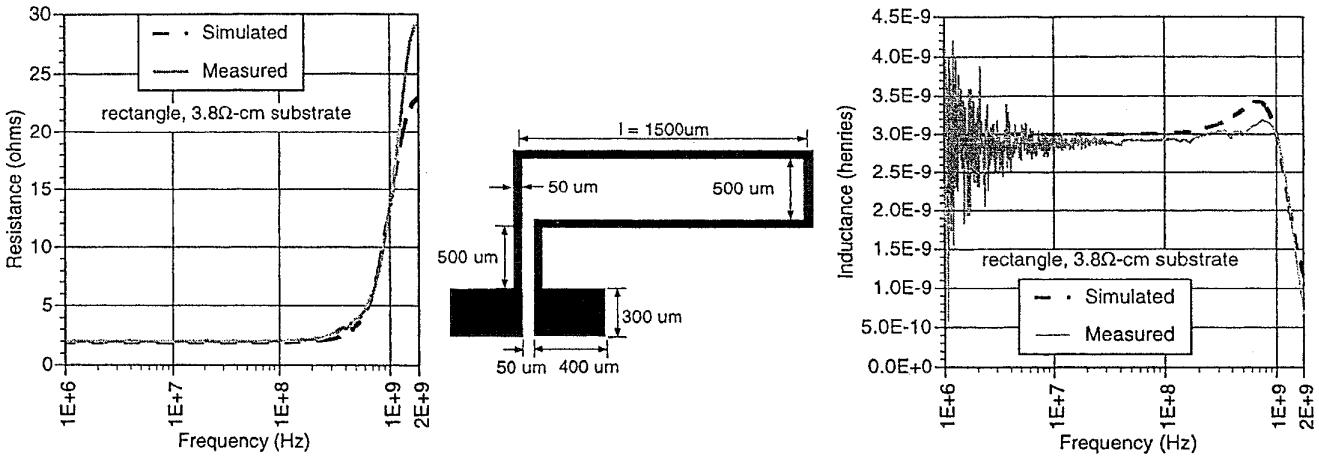

Figure 5: Comparison between simulation and measurement for rectangular test structure on low resistivity (3.8Ω-cm) substrate. Comparison between calculated and measured results on high resistivity (20Ω-cm) substrate also showed excellent agreement (not shown here due to space constraints).

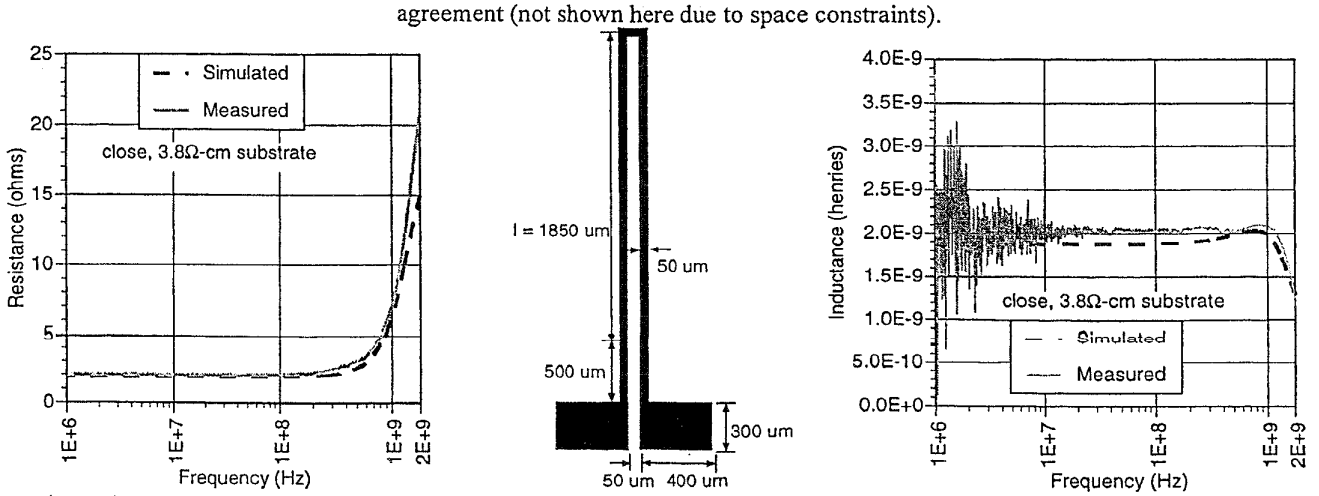

Figure 6: Comparison between simulation and measurement for closely spaced lines on low resistivity (3.8Ω-cm) substrate. Comparison between calculated and measured results on high resistivity (20Ω-cm) substrate also showed excellent agreement (not shown here due to space constraints).